Catena 182 (2019) 104132

Contents lists available at ScienceDirect

Catena

journal homepage: www.elsevier.com/locate/catena

Changes in sediment load in a typical watershed in the tableland and gully region of the Loess Plateau, China

Guo Qiankun[a,b], Ding Zhaowei[c], Qin Wei[a,b,*], Cao Wenhong[a,b], Lu Wen[a,b], Xu Xiaomei[d], Yin Zhe[a,b]

[a] State Key Laboratory of Simulation and Regulation of Water Cycle in River Basin, China Institute of Water Resources and Hydropower Research, Beijing 100048, PR China

[b] Research Center on Soil and Water Conservation of the Ministry of Water Resources, Beijing 100048, PR China

[c] State Key Laboratory of Urban and Regional Ecology, Research Center for Eco-Environmental Sciences, Chinese Academy of Sciences, PR China

[d] Xifeng soil and water conservation experimental station, Yellow River Conservancy Commission of the Ministry of Water Resources, PR China

ARTICLE INFO

Keywords:
Sediment load change
Influencing factors
Sediment delivery ratio
Soil erosion
Check dams

ABSTRACT

Changes in sediment load of the Yellow River, and the contributing factors, have been widely studied and many valuable results have been reported. However, these studies were mainly conducted in the hill and gully region of the Loess Plateau, while studies on other regions, such as the tableland and gully region, which is more important for food production, and social and economic development, have rarely been reported. In this study, a typical watershed in this region was selected to analyze the changes in the sediment load between 1981 and 2016, and the contributions of its influencing factors. The Mann-Kendall (MK) test was applied to annual runoff and sediment load, and the year 1994 was identified as the year of mutation; thus, a baseline period (1981–1994) and a response period (1995–2016) were distinguished. By combined use of the Revised Universal Soil Loss Equation (RUSLE) and the Sediment Delivery Distributed Model (SEDD), sediment yields for the two periods were estimated, and compared with the corresponding measured data. The contributions of influencing factors, including natural factors (changes in rainfall and rainfall erosivity) and anthropogenic activities (human induced vegetation change, slope terraced farmlands, and check dams in the stream networks), were analyzed. The results demonstrate that: 1) Sediment load in Yanwachuan watershed decreased substantially between the two periods; 2) Sediment load change was mainly influenced by human induced vegetation cover changes across the watershed, and check dams in the stream networks, which accounted for approximately 80% and 20% of the sediment load reduction, respectively; 3) The sediment trapped by the check dams are likely to increase in the future, thus effective measures should be implemented to protect check dams, and to ensure the effects of check dams on sediment reduction can be maximized. The results of this study help to understand the changes in sediment load in the tableland and gully region, and can provide valuable guidance on best practices in terms of local soil conservation management.

1. Introduction

Due to the coupled effects of global climatic change and human activities, sediment loads of the world's rivers have reduced by 50% in recent decades (Walling and Fang, 2003; Wang et al., 2015a). For example, dam construction and river diversion for irrigation, industrial and municipal uses have effectively trapped most of the sediments in the Colorado River (Carriquiry and Sanchez, 1999). In the late 1980s, the globally cumulative sediment load intercepted by reservoirs was estimated to be 1.5 Gt a^{-1}, equivalent to 7.5–10% of the total natural river monthly flux (Meybeck, 1988); more recently, Vörösmarty et al. (2003) estimated that 28% of total sediment load was intercepted by reservoirs based on a comprehensive survey of basin watershed. Syvitski et al. (2005) concluded that anthropogenic influences have increased sediment transport by increasing soil erosion (2.3 ± 0.6 Gt a^{-1}), while reducing the sediment flux reaching the world's coast (1.4 ± 0.3 Gt a^{-1}) due to the retention by reservoirs. Understanding the drivers and mechanisms behind the changes in sediment load is crucial for developing strategic plans for the sustainable management of catchments (Montgomery, 2007).

* Corresponding author at: State Key Laboratory of Simulation and Regulation of Water Cycle in River Basin, China Institute of Water Resources and Hydropower Research, Beijing 100048, PR China.
E-mail address: qinwei@iwhr.com (Q. Wei).

https://doi.org/10.1016/j.catena.2019.104132
Received 4 July 2018; Received in revised form 3 June 2019; Accepted 16 June 2019

In China, numerous studies have focused on the effects of climate and human activities on runoff and sediment load changes in many important rivers (Miao et al., 2011), such as the Lancang-Mekong River (Liu et al., 2013), Yalungtsangpo-Brahmaputra River (Wen et al., 2002), Nujiang-Salween River (Liu and He, 2013), and Yili-Balkhash River (Deng et al., 2011). Runoff and sediment transportation modules in 10 main seagoing rivers in China have been analyzed by Liu et al. (2007), with results indicating that the sediment transport of almost all rivers had been substantially reduced, with the main cause being anthropogenic activities, such as dams, reservoirs, and watershed soil and water conservation measures. The change in sediment load of the Yangtze River, the largest river in China and the third largest river worldwide, has been widely studied, with most studies indicating that anthropogenic activity has been the dominant factor in the changes in sediment load of the river and its main tributaries. Among these, dam trapping ranked first, followed by climate change, sand extraction and soil conservation measures (Chen et al., 2001; Chen et al., 2005; Yang et al., 2005; Yang et al., 2006; Zhang et al., 2006; Chen et al., 2008; Dai et al., 2008; Dai and Lu, 2014).

Sediment load in the Yellow River, the second largest river in China, has decreased substantially from 1.6 Gt a^{-1} to < 0.1 Gt a^{-1} over the past 60 years (Yellow River Conservancy Commission of Ministry of Water Resources in China, 2016). Studies on changes in sediment load and the contributions of influencing factors for the Yellow River and its tributaries are listed in Table 1. These studies again demonstrate that sediment reduction was predominantly caused by human activities, such as soil conservation measures and reservoir retention. However, some details are yet to be resolved, which restricts our understanding of the factors that influence changes in sediment load in the Yellow River Basin.

First, these studies are mainly conducted on the large watershed scale (usually > 1000 km^2 in China), while studies on medium (usually 100–1000 km^2) or small (< 100 km^2) watersheds are uncommon. This is a limitation, since in the Loess Plateau, soil conservation and watershed management is usually conducted on the small or medium watershed scale, so data collected from larger watersheds are associated with more uncertainties. Thus, an understanding of the changes in sediment load in small or medium watersheds is important for future soil conservation strategies. Table 1 also shows that very few studies have been performed beyond the hill and gully region of the Loess Plateau, despite this region accounting for the majority of the Loess Plateau. Relevant studies on other regions are also important, especially for the tableland and gully region, which covers a large area of about 2×10^5 km^2 in Gansu, Shaanxi and Shanxi Provinces in China, and plays an important role in social and economic development, and food production, due to superior natural conditions (e.g., large area of tableland, temperate climate) compared to the hill and gully region (Zhu, 1953). According to historical reports (Dong, 2005), severe soil erosion events have occurred more frequently in the tableland and gully region than the hill and gully region, and caused adverse consequences ranging from the loss of arable land to huge economic losses, and even injury and loss of life. The severity of these consequences is probably due to the unique erosion characteristics of the soil in this region. In the tableland and gully region, the large amount of runoff on the tablelands produced by extreme precipitation events usually has the destructive power to detach and transport slope soil as it flows from the high tablelands to the deep valleys (Zhu, 1954; Xing et al., 1991; Li et al., 1993; Tian et al., 2008). This has resulted in severe erosion, leading to natural disasters in Xixian County (Yang et al., 1989), Xifeng District (Li et al., 1993), Qianxian County (Xue, 1995), Qingcheng County (Wang et al., 2005), Huachi County, and Huanxian County (Zhang et al., 2015a, 2015b), among others. Thus, studies on changes in sediment load of the tableland and gully region are of great significance. However, despite some studies having noted changes to sediment load in this region (Wang et al., 2015b), no quantitative evaluation of the factors affecting sediment load changes has so far been reported. Further studies are therefore required to help inform best practice on soil erosion control and soil conservation management in the tableland and gully region.

Second, the most widely used method for analyzing the effects of factors on that influence sediment load is the double mass curve method (Table 1), proposed by Merriam (1937). It is a simple, visual, and practical method that is used to study the consistency and long-term trends of hydro-meteorological data (Mu et al., 2010), assuming the relationships between sediment load and rainfall are proportional. However, the relationships between runoff or sediment load and rainfall are usually not proportional (Mu et al., 2010). Because of this, some researchers have attempted to analyze the contributions of influencing factors by the model simulation method: usually by the combined use of soil erosion models and sediment delivery models (Zuo et al., 2016; Zhao et al., 2017). Soil erosion models can be classified into two types: physically-based and empirical models (Merritt et al., 2003). Although physically-based models are more likely to yield reliable predictions (Wainwright and Mulligan, 2013), complex parameters that cannot be easily and precisely quantified are required, making expected ideal results difficult to obtain (Kinnell, 2000; Perrin et al., 2001). In lieu of this, empirical models are widely used, and have been applied to rivers in the USA (Williams and Berndt, 1977; Wilson, 1986), Canada (Mellerowicz et al., 1994), Belgium (Gabriels et al., 2003), and Italy (Amore et al., 2004). In most cases, empirical models such as RUSLE (Revised Universal Soil Loss Equation), and MUSLE (Modified Universal Soil Loss Equation), produce sound predictions in the Loess Plateau (Li et al., 2017). In sediment delivery models applied to China, especially in the Loess Plateau, sediment delivery ratios have mainly been estimated by empirical equations based on watershed parameters such as area, gully density, and runoff coefficients (Gong and Xiong, 1979; Mou and Meng, 1982; Cao et al., 1993; Chen, 2000; Xu, 2010); thus, these localized equations cannot be easily extended to other watersheds. The most widely used sediment delivery model is the sediment delivery distributed (SEDD) model (Ferro and Porto, 2000), which integrates the main factors influencing sediment transport, such as velocity (McCuen, 1998), time (Jain and Kothyari, 2000), and path (USDA Soil Conservation Services, 1975). This model can also reflect the effect of land use and vegetation changes on sediment delivery ratio (SDR; Ferro and Porto, 2000). The SEDD model has often been used in conjunction with the Revised Universal Soil Loss Equation (RUSLE) (Renard et al., 1997) to acquire watershed scale sediment load such as in Cho and Jeoung (2005); Fernandez et al. (2003); Fu et al. (2006); Kamaludin et al. (2013); Taguas et al. (2011) and Yang et al. (2007). In summary, model simulations appear to be better than the double mass curve method for studying changes in sediment load, since a proportional relationship between parameters is not necessary. However, such simulations have rarely been applied to the tableland and gully region of the Loess Plateau.

To address the gaps in our understanding of the factors that influence changes in sediment load in the Yellow River Basin, a typical medium-sized watershed in the tableland and gully region, Yanwachuan watershed, was selected. Changes in sediment load and the influencing factors were determined by the combined methods of RUSLE and SEDD. The objectives of this study were: 1) to detect changes in sediment load in the Yanwachuan watershed; 2) to evaluate the quantitative contributions of influencing factors on changes in sediment load.

2. Materials and methods

2.1. The study area

The Yanwachuan watershed is a medium watershed of the Malianhe River, a first-order tributary of Jinghe River, and second-order tributary of the Yellow River. The watershed is located in Qingyang, Gansu Province, China (Fig. 1), and covers an area of 369 km^2 with elevation

Table 1
Studies on changes in sediment load and the contributions of influencing factors in Yellow River and its tributaries.

Rivers	Hydrologic station[a]	Period[b]	Influencing factors and contribution[c]	Reference
Yellow River	LZ, TDG, HYK, LJ	I: 1950–1978; II:1979–2005	Precipitation: 30%; Reservoir operation in upper reaches: 10%; Soil conservation: 40%; Reservoir retention: 20%;	Wang et al., 2007a
Yellow River	TNH, LZ, HK, LM, SMX, HYK, LJ	I: 1950s–1969; II:1970–2008	Climate change: 46%; Human activities: 54%	Miao et al., 2011
Yellow River	TDG, HYK	I:1950s–1984; II:1985–2008	Water extraction diversion: 12%; Reservoir siltation: 35%; Soil Conservation Measures: 53%	Gao et al., 2011
Yellow River, Weihe, Fenhe, Wudinghe	TDG, LM, HYK, Hejin, Huaxian, Baijiachuan	I:1950s–1969; II:1970–2009	Climate change, rainfall, soil and water conservation measures, and other human activities. Contribution ratios were not provided	Zhao et al., 2012
The Loess Plateau	TNH, LZ, TDG, LM, TG, HYK, GC, LJ	I:1951–1979; II:1980–1999; III: 2000–2010 P3:2000–2010	Perennial vegetation cover: 10% (II), 57% (III); Terrace farming: 33% (II), 17% (III); Check dams: 21% (II), −9% (III); Other factors: human water consumption, sand extraction, climate change	Wang et al., 2015a
Huangfuchuan	–	I:1954–1982; II:1983–2000	Soil Conservation Measures: 87%; Precipitation: 13%	Rustomji et al., 2008
Gushanchuan	–	I:1954–1979; II:1980–2000	Soil Conservation Measures: 37%; Precipitation: 63%	Rustomji et al., 2008
Kuyehe	–	I:1954–1979; II:1980–2000	Soil Conservation Measures: 79%; Precipitation: 21%	Rustomji et al., 2008
Jialuhe	–	I:1954–1977; II:1978–2000	Soil Conservation Measures: 70%; Precipitation: 30%	Rustomji et al., 2008
Shiwanghe	–	I:1959–1982; II:1983–2000	Soil Conservation Measures: 74%; Precipitation: 26%	Rustomji et al., 2008
Xinshuihe	–	I:1959–1979; II:1980–2000	Soil Conservation Measures: 45%; Precipitation: 55%	Rustomji et al., 2008
Sanchuanhe	–	I:1957–1978; II:1979–2000	Soil Conservation Measures: 80%; Precipitation: 20%	Rustomji et al., 2008
Weifenhe	–	I:1956–1981; II:1982–2000	Soil Conservation Measures: 89%; Precipitation: 11%	Rustomji et al., 2008
Zhujiahe	–	I:1957–1982; II:1983–2000	Soil Conservation Measures: 87%; Precipitation: 13%	Rustomji et al., 2008
Coarse Sandy Hilly Region	–	I:1954–1979; II:1980–2000	Soil Conservation Measures: 46%; Precipitation: 54%	Rustomji et al., 2008
Yanhe	Ganguyi	I:1965–1971; II:1972–1976; III:1977–1986; IV:1987–1996; V:1997–2001	Human activities: 63.4% (II), 47.0 (%III), 23.4% (IV), 67.2% (V)	Wang et al., 2007b
Yanhe	Ganguyi	I:1961–1973; II:1974–1996; III:1997–2008	Rainfall: −17.6% (II), 14.6% (III) Human activities: 117.6% (II), 85.4% (III)	Ren et al., 2012
Wudinghe	–	I:1957–1971; II:1972–1996	Soil Conservation Measures: 64%; Precipitation: 36%	Rustomji et al., 2008
Wudinghe	Baijiachuan	I:1956–1969; II:1970–1996	Rainfall: 52.1%; Soil Conservation Measures: 47.9%	Xu, 2004
Wudinghe	Baijiachuan	I:1956–1971; II:1972–1979; III:1980–1989: IV:1990–1999 V: 2000–2006	Rainfall: 20.2% (II), 19.6% (III), 28.2% (IV), 11.1% (V) Human activities: 79.8% (II), 80.4% (III), 71.8% (IV), 88.9% (V)	Gao et al., 2009
Huangfuchuan	Huangfu	1991–2009	Land use changes: 31.4%; check dams: 51.9%	Zhao et al., 2017
Huangfuchuan	Huangfu	1954–2012	Land use changes: 81.0%; climate changes: 40.6%	Zuo et al., 2016

[a] GC: Gaocun; HK: Hekou; HYK: Huayuankou; LJ: Lijin; LM: Longmen; LZ: Lanzhou; TDG: Toudaoguai; TG: Tongguan; TNH: Tangnahai, SMX: Sanmenxia.
[b] Period I is the baseline period for analyzing the changes in sediment load, and the contribution of influencing factors from Period II to Period V.
[c] The method used in all the studies in this table was the Double Mass Curve method, except for Rustmoji et al., 2008, Zhao et al., 2017, and Zuo et al., 2016, which used a linear regression model between the square root of annual sediment yield and runoff and a dummy variable, the sediment delivery distributed model (SEDD), and the soil and water assessment tool (SWAT), respectively.

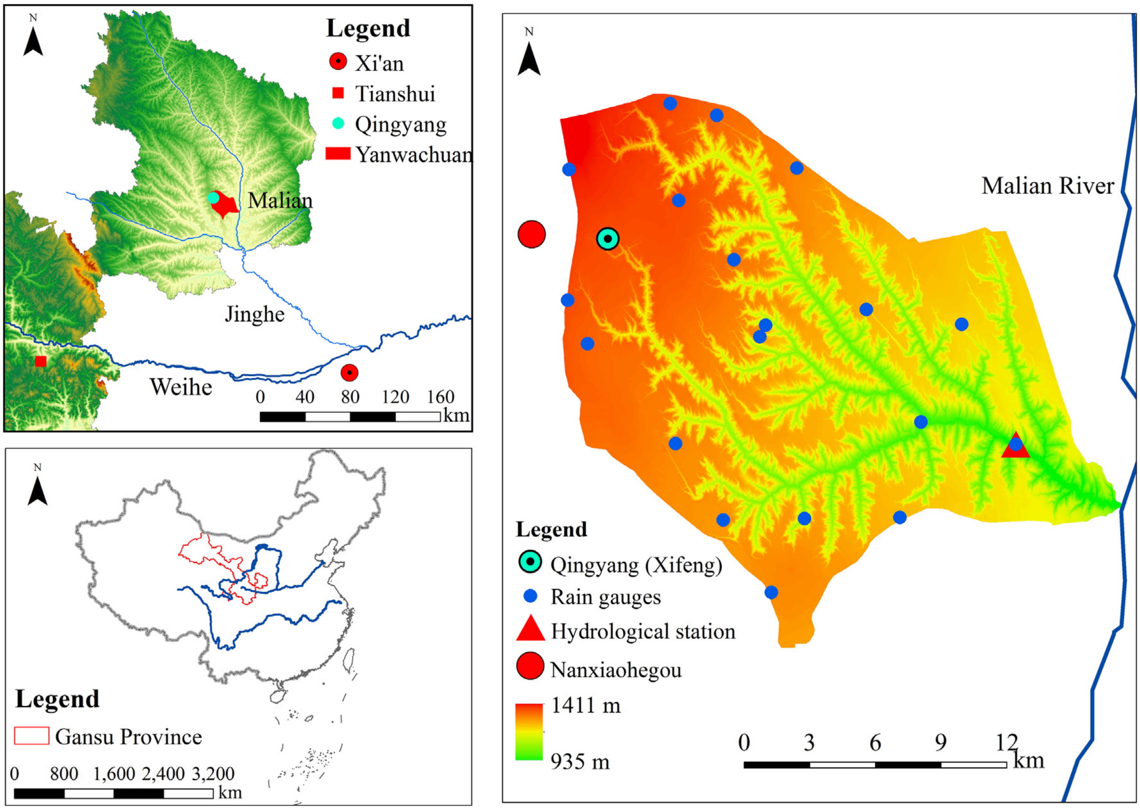

Fig. 1. Geographical distribution of the Yanwachuan watershed, rain gauges and hydrometric station.

ranging from 935 m to 1411 m. The soils are mainly dark loessial soil (Calcarid Regosols, FAO) in the tablelands, typical loessial soil (Calcic Cambisols, FAO) on the slopes and alluvial soil (Calcaric Fluvisols, FAO) in the gullies, accounting for 47.3, 42.7 and 10.0% of the total watershed, respectively. According to data recorded at the nearby Xifeng meteorological station for 1937–2009, the annual rainfall is 542 mm, of which 68% falls from July to September in the form of torrential rains. The land uses in the watershed are mainly farmland, forest and grassland, of which the farmlands are mainly on the tablelands, while the forests and grasslands are situated on the slopes and in the gullies.

According to historic records, soil conservation management in the Yanwachuan watershed was initiated fragmentarily from 1950, while large scale watershed management was not implemented until 1975. However, watershed management has stagnated from 1979, since land has been contracted to local farmers, meaning soil conservation measures, including engineering and biological measures, progressed slowly during the 1980s and the early 1990s. Many soil conservation programs have been implemented since 1994, such as the World Bank Loan Project on soil and water conservation in the Loess Plateau (1994), the “Converting slope farmland to forest” Project implemented by Chinese Government (1999), and the watershed management projects in the new decades.

A hydrometric station (Fig. 1) was built in 1975 at Xifeng experimental station of soil and water conservation, which belongs to the Yellow River Conservancy Commission, the Ministry of Water Resources of China. The controlled area of the station was 326 km^2, which comprises 88.2% of the Yanwachuan watershed. Daily flow charge and sediment load was measured at the Yanwachuan hydrometric station, using a parabolic weir. Water levels were measured four times each day (at 02:00, 08:00, 14:00 and 20:00), and the flow charge was estimated according to the water level–flow discharge relationship. The sediment concentration was also measured four times each day. On most days, the sediment samples were collected manually at the midstream of the flow to be better representative of the suspended sediment. During flood events, the sediment concentration was usually very high and could be considered as a hyper-concentrated flow, which is a characteristic feature of the Loess Plateau (Hessel, 2006), and quite different from the normal streamflow for most rivers. A hyper-concentrated flow is a uniform flow with a high suspended fine-material concentration, and a viscosity greater than that of water (Rickenmann, 1991). Sediment collected at seven hydrometric stations at six first-order tributaries of the Yellow River (Zhao and Niu, 1983) and Ninghua station in northern Shanxi province (Li, 2005) all indicated that in the Loess Plateau, during hyper-concentrated flow, both the vertical distribution and the cross-sectional distribution of sediment concentration are uniform. Sediment samples were collected many times during flood events, to accurately resolve rapid changes in sediment concentration with time.

Daily rainfall data was measured from 19 rainfall gauges distributed throughout the watershed. Cross sections were used to record the height of sediment trapped by check dams before the rainy season (usually in May) and after the rainy season (usually in September) each year, or after flood events. The cross sections were taken from the head, middle and tail of the dams, since sediment height usually differed at different sites. Sediment trapped by the check dams during the rainy season was estimated from these data. Similar measurements were also recorded across 1981–2004 and 2008–2013 at Xifeng experimental station. The cross-sectional method has been widely used to measure sediment trapped by small check dams in the Loess Plateau for decades, as it is cheap and effective (Yang, 2003). The accuracy of recorded heights has been improved by using GPS, with the error associated with measured heights at the same point being only about 3 mm (Ai et al., 2005). Land use and vegetation cover data for different periods were acquired based on remote sensing images and a 5-m resolution digital elevation model (DEM) was also acquired. Types of data recorded are listed in Table 2.

Table 2
Summary of data collected from the Yanwachuan Watershed.

Data	Information
Topography	5 m resolution DEM, field verified
Rainfall[a]	Daily data from 19 rainfall gauges in the watershed from 1981 to 2016
Hydrology	Daily runoff and sediment load data from hydrologic station from 1981 to 2016
Landuse[b]	5 m resolution in 2008 and 2010 (field verified), 30 m in 1990, 2000, 2010 and 2015
Vegetation[c]	30 m resolution Landsat-TM/ETM + remote sensing images

[a] Not measured for some rainfall gauges in the 1990s.
[b] The 5 m data was acquired from Xifeng station, while the 30 m data was extracted from national land use change records. Total area calculated for each land use type from 5 m and 30 m data in 2010 were similar.
[c] http://glovis.usgs.gov. The selected dates were 1986.07.24, 1991.08.23, 2000.07.30, 2009.07.23 and 2017.07.13.

2.2. Estimation of soil erosion

Based on the measured hydrological data, temporal changes in annual sediment yield were analyzed by the Mann-Kendall (MK) trend test. The nonparametric MK statistical test is widely used to identify monotonic trends in hydro-meteorological data such as temperature, precipitation, and stream flow, since it is suitable for non-normally distributed, censored, and incomplete data, which are frequently encountered in hydrological time series (Yue et al., 2002). In the Yanwachuan watershed, a non-significant decreasing trend was detected for 1981–2016 with an inflection point occurring in approximately 1994 (Fig. 2; Fig. 3). Thus, a baseline period (1981–1994), and a response period (1995–2016), were distinguished for analyzing sediment load change, and the contributions of its influencing factors.

In this study, the empirical soil erosion model RUSLE was used to calculate the average annual soil erosion for the baseline and response periods. The equation used was:

$$M = 100RKLSCP \tag{1}$$

where M is the average annual soil erosion, t km^{-2} a^{-1}; R is the rainfall erosivity, MJ mm hm^{-2}h^{-1} a^{-1}; K is the soil erodibility, t ha h ha^{-1} MJ^{-1} mm^{-1}; L is the slope length factor; S is the slope gradient factor; C is the cover management factor; and, P is the support practices factor.

2.2.1. Estimation of rainfall erosivity factor (R)

In RUSLE, rainfall erosivity (the R factor) is calculated by multiplying the total storm energy by the maximum 30-min intensity. However, the high temporal resolution continuous rainfall data series required by the equation are rarely available in the Yanwachuan watershed, thus daily rainfall data have been used to estimate rainfall erosivity, as documented in previous studies (Zhang et al., 2003; Xie et al., 2016). In the Loess Plateau, the daily rainfall model proposed by Xie et al. (2016) can generate reasonable approximations of the annual R factor, with a symmetric mean absolute percentage error < 11%. This model has therefore been widely used for estimating rainfall erosivity:

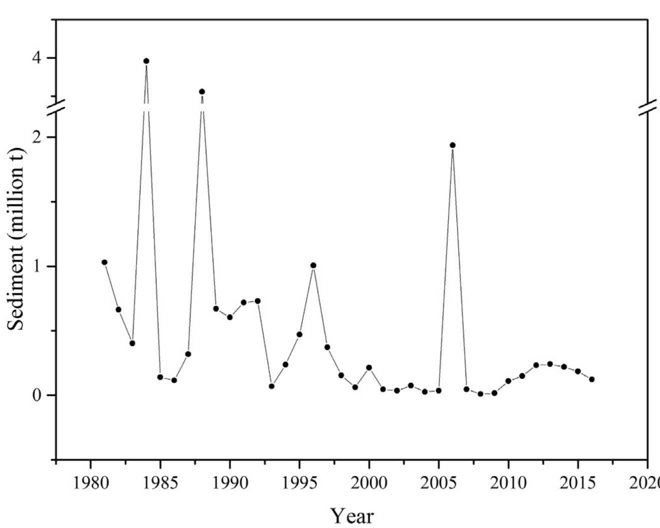

Fig. 2. Annual measured sediment in the Yanwachuan watershed from 1981 to 2016.

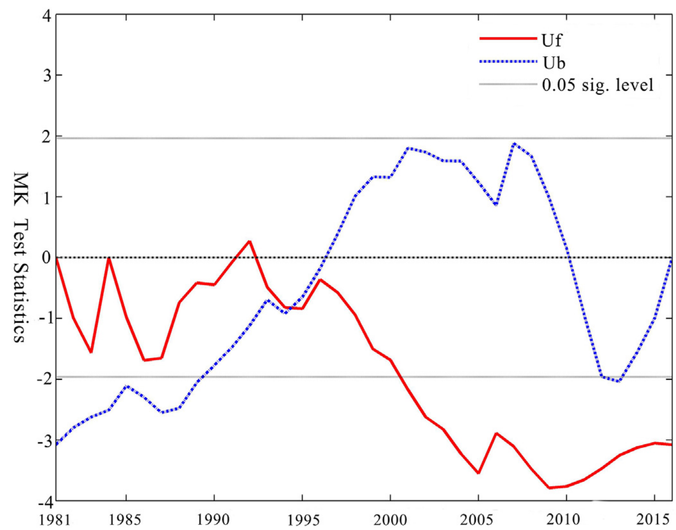

Fig. 3. MK trend test for annual sediment in the Yanwachuan watershed (Uf: Forward Sequence; Ub: Backward Sequence).

$$R_{day} = \alpha P_d^{1.7265} \tag{2}$$

where P_d is the daily rainfall, mm, and is equal to the actual rainfall when > 9.7 mm or equal to 0 when < 9.7 mm; α is a parameter that equals 0.39 in the warm season (May to September) and 0.31 in the cool season (October to April). The annual rainfall erosivity for each gauge can be acquired by summing the corresponding daily rainfall erosivity measured throughout the year, and the spatial distribution of rainfall erosivity for both the baseline and response periods can be interpolated using the inverse distance weighted (IDW) method in the ArcGIS environment.

2.2.2. Estimation of soil erodibility factor (K)

In the Yanwachuan watershed and the nearby Nanxiaohegou watershed (Fig. 1), > 100 runoff plots have been established by the Xifeng soil and water conservation experimental station since 1954, to measure soil losses for various land use types, including slope farmland, forest, grassland, etc. However, there were no fallow plots in these two watersheds, suggesting that it may be inaccurate to estimate K values from local plot data. Currently, the K values estimated via the Wischmeier formula (Wischmeier et al., 1971) and the EPIC (Erosion Productivity Impact Calculator) formula (USDA, 1990) are substantially higher than the K values estimated from runoff plot data in the Loess Plateau (Zhang et al., 2004; Zhang et al., 2015a, 2015b), implying that neither method can be directly applied to the Loess Plateau. Zhang et al. (2004, 2015a, 2015b) reported that K values estimated via EPIC were 3.36, 2.59, 6.32 and 3.34 times greater than the K values recorded at runoff plots in Zizhou, Suide, Ansai, and Lishi, respectively. All these plots were located in the Loess Plateau, and yielded a mean correction factor of 3.90. Thus, in this study, the K values estimated via EPIC for different soil types were divided by 3.90 to produce the final K value used. The EPIC equation is:

$$\mathrm{K} = \{0.2 + 0.3\exp[-0.0256\mathrm{SAN}(1 - \mathrm{SIL}/100)]\} \times \left(\frac{\mathrm{SIL}}{\mathrm{CLA} + \mathrm{SIL}}\right)^{0.3} \times \left[1 - \frac{0.25SOC}{SOC + exp(3.72 - 2.95SOC)}\right] \times \left[1 - \frac{0.7SN_1}{SN_1 + exp(-5.51 + 22.9SN_1)}\right]/7.59 \tag{3}$$

where, SAN is the soil sand content, %; SIL is the soil silt content, %; CLA is the soil clay content, %; SOC is the soil organic carbon content, %; and $SN_1 = 1 - SAN/100$. For dark loessial soil (Calcarid Regosols, FAO), the percentages of SAN, SIL, CLA and SOC were 12.2, 62.7, 25.1 and 0.63%, respectively; for typical loessial soil (Calcic Cambisols, FAO), the same percentages were 12.5, 60.4, 27.1 and 0.84%, respectively; and for alluvial soil (Calcaric Fluvisols, FAO), they were 57.5, 31.2, 11.3 and 1.54%, respectively. Soil properties were measured in the lab from soil samples collected in the field. The measured soil properties were then validated according to soil inventory data (Soil inventory office in Qingyang, 1989; Geng, 2011). Finally, the spatial distribution of K values was derived from the spatial distribution of soil types in the Yanwachuan watershed.

2.2.3. Estimation of the slope length and gradient factor (L and S)

The slope length factor (L) and slope gradient factor (S) represent the effect of topography on soil erosion. The LS factor is usually computed based on DEM data for watershed scale applications. In this study, an LS software tool developed by Fu et al. (2015), which has been widely used for soil erosion estimation in China, was used to acquire the geographical distribution of the L and S factors. The equations used in this tool for estimating the S factor were:

$$S = 10.8sin\theta + 0.03 \quad \theta < 5° \tag{4}$$

$$S = 16.8sin\theta - 0.5 \quad 5° < \theta < 10° \tag{5}$$

$$S = 21.91sin\theta - 0.96 \quad \theta \geq 10° \tag{6}$$

where Eqs. (4)–(5) were taken from McCool et al. (1989) and eq. (6) from Liu et al. (1994). S is the slope gradient factor, and θ is the slope gradient, °, acquired from the 5 m resolution DEM.

The L factor was calculated based on the contributing area method developed by Desmet and Govers (1996), and the equations were:

$$L_{i,j} = \frac{(A_{i,j} + D^2)^{m+1} - A_{i,j}{}^{m+1}}{D^{m+2}x_{i,j}{}^m(22.13)^m} \tag{7}$$

$$x_{i,j} = cos\,\gamma_{i,j} + sin\,\gamma_{i,j} \tag{8}$$

where, $A_{i,j}$ is the contributing area at the inlet of a grid cell with coordinates (i, j), m^2; D is grid cell size, m, $x_{i,j}$ is the contour length coefficient for the grid cell with coordinates (i, j); $\gamma_{i,j}$ is the aspect direction of the grid cell with coordinates (i, j); 22.13 is the slope length of a unit runoff plot, m; and m is the slope length exponent, which is 0.5 for slopes > 5%, 0.4 for slopes > 3% and ≤ 5%, 0.3 for slopes > 1% and ≤3%, and 0.2 for slopes ≤1%.

2.2.4. Estimation of crop and management factor (C)

The C values in the Yanwachuan watershed were quantified based on various land use types. For vegetation types, such as forest, shrub land and grassland, C values were estimated according to the equation established from the runoff plot data in the Loess Plateau by Jiang et al. (1996):

$$C = e^{-0.0418(V-5)} \tag{9}$$

where, C is the crop and management factor; V is vegetation cover (%), estimated from Landsat-TM/ETM+ remote sensing images downloaded from the United States Geological Survey (USGS) (Table 2), using the following equations:

$$V = (NDVI - NDVI_{min})/(NDVI_{max} - NDVI_{min}) \tag{10}$$

$$NDVI = (NIR - RED)/(NIR + RED) \tag{11}$$

where, NIR is the near infrared band and RED is the red light band (both these variables were estimated in the ENVI environment based on Landsat-TM/ETM+ remote sensing images); $NDVI$ is the normalized difference vegetation index; and $NDVI_{min}$ and $NDVI_{max}$were the minimum and maximum values of $NDVI$ in the Yanwachuan watershed. The spatial distribution of C values of vegetation types in the baseline and response periods can be determined using Eqs. (9)–(11).

For agricultural land, the main cropping system in the Yanwachuan watershed is winter wheat with summer fallow. Summer crops such as maize, soybean and millet are only planted in relatively small proportions on agricultural lands. Runoff plot data measured at the nearby Tianshui soil and water conservation experimental station (Fig. 1), has used to calculate C values for winter wheat, maize, soybean, and millet of 0.23, 0.28, 0.51 and 0.53, respectively (Zhang et al., 2001). The C values for crops in Tianshui could be used in this study due to similar natural conditions and cropping systems there and in the Yanwachuan watershed. Since the dominant crop in the Yanwachuan watershed is winter wheat, the C value of agricultural lands is quantified as 0.23 in this study. C values of water bodies and construction sites were quantified as 0 and 1, respectively, based on relevant studies in the Loess Plateau (Gao et al., 2015).

2.2.5. Estimation of soil conservation practice factor (P)

Farmland terracing is the main soil conservation technique practices on slopes in the Yanwachuan watershed. The value of P was calculated to be 0.05 using long-term field measurements from runoff plots in the nearby Nanxiaohegou watershed (Tian et al., 2008). However, the P factor of RUSLE model is usually overestimated when values measured from plot scale are directly applied to larger areas (catchment or regional scale) and P values in longer slopes are 1.2 to 2.7 times large than on small plots (Zhao et al., 2019). Thus this study applies that P value of 0.1 (2 times of the value of 0.05 measured at nearby plots) to terraced farmland in the Yanwachuan watershed. A P value of one was used for other land use types.

2.3. Estimation of sediment yield

In the Yanwachuan watershed, soil conservation management practices in the baseline period (1981–1994) stagnated. The effect of soil conservation measures, such as terraced farmland, check dams, etc., on sediment yield was therefore negligible in the baseline period when compared with the response period, meaning sediment transport in the baseline period can be approximately considered as a natural process. Thus, the SDR for the baseline period is calculated by Eq. (12):

$$SDR_b = Y_b/A_b \tag{12}$$

where, SDR_b is the sediment delivery ratio for the baseline period; Y_b is the average annual measured sediment yield for the baseline period, t; A_b is the estimated average annual soil erosion in the baseline period for the control area of Yanwachuan hydrologic station, t, which is estimated by Eq. (1).

In this study, the estimated sediment yield in the response period (1995–2016) is calculated by:

$$Y_{re} = SDR_{re}A_r \tag{13}$$

where, Y_{re} is the estimated average annual sediment yield for the response period, t; SDR_{re} is the estimated sediment delivery ratio for the response period; and A_r is the estimated average annual soil erosion, t, for the response period. The SDR_{re} and its spatial distribution can be quantified using eqs. (14–16):

$$SDR_i = exp(-\mu t_i) \tag{14}$$

where, SDR_i is the fraction of the gross soil loss from grid cell i that actually reaches a continuous stream system; μ is a watershed-specific parameter; t_i is the travel time from the grid cell i to the nearest channel cell, h. If the flow path from the grid cell i to the nearest channel traverses N_p cells, the travel time for cell i is calculated by adding the travel time for each of the N_p cells located along the flow path:

$$t_i = \sum_{i=1}^{N_p} d_i/v_i \tag{15}$$

where, d_i is the length of the grid cell i along the flow path, m, which is equal to the side length of the grid cell when the flow direction is north, east, south and west, or is equal to the diagonal length of the grid cell when the flow direction is northeast southeast, southwest and northwest; and v_i is the flow velocity of the grid cell i, m·s^{-1}, which is calculated using Manning's equation:

$$v_i = 1.486\frac{R_h{}^{\frac{2}{3}}}{n}s_i{}^{0.5} \tag{16}$$

which can be simplified as:

$$v_i = k_i s_i{}^{0.5} \tag{17}$$

where, R_h is the hydraulic radius, ft.; n is the roughness coefficient; s_i is the slope gradient of the grid cell i, m·m^{-1}, and is quantified based on the 2.5 m resolution DEM; and k_i is a coefficient dependent om surface cover herein named velocity coefficient for the grid cell i, m·s^{-1} (Haan et al., 1994; Smith and Maidment, 1995; McCuen, 1998). The minimum value of s_i was set as 0.003 in this study to ensure the lower limit of velocity in the watershed (Fernandez et al., 2003).

To calculate the SDR_{re}, the parameters k, μ and the stream networks of the watershed must first be quantified. The stream networks are the pathways for sediment transportation. In this study, multiple threshold areas for stream networks (0.01, 0.025, 0.05, 0.1, 0.25, 0.5, 1.0, 2.5 and 5.0 km^2) were used to estimate the corresponding lengths of river nets, and determine the relationship between threshold areas and total lengths of river nets. The suitable threshold area was chosen when the total river net lengths began to remain the same. The corresponding stream networks were then determined to estimate the spatial distribution of SDR. According to the different threshold areas and the corresponding lengths of stream networks in the Yanwachuan watershed, the relationship can be quantified as:

$T_l = 263.94D_t{}^{-0.481}$ (R2 = 0.99) (18)where, T_l is the total length of stream networks, km; and D_t is the threshold area, km^2. The total lengths tended to remain stable when a threshold area of 0.25–0.5 km^2 was used, thus the threshold area was quantified as 0.25 km^2, and the corresponding stream networks were used for estimating SDR.

The k values for sparse forest, dense forest, shrub land, sparse grassland, dense grassland, residential land, conventional tillage, contour tillage and water body were quantified as 0.43, 0.21, 0.43, 0.64, 0.46, 6.28, 2.77, 1.401 and 0 m s^{-1}, respectively. These values were taken from various sources in the literature, such as Haan et al. (1994), Smith and Maidment (1995), McCuen (1998) and Fernandez et al. (2003). As indicated, land use and vegetation cover have changed substantially between the two periods; thus, the k values may change as a consequence. For forest cover, young trees were planted during the response period, and a period of several years is needed for them to reach relatively constant coverage, while the forest in the baseline period was mainly fully grown despite less coverage. For this reason, the forest k value for the baseline period was calculated assuming dense coverage, while in the response period it was calculated assuming sparse coverage for the new planted forest and dense coverage for grown forest. For grassland, restoration periods are much shorter than for forests, and the vegetation cover in the response period was much higher than in the baseline period, thus the k value for grassland in the baseline period was calculated assuming sparse coverage, while in the response period it was calculated assuming dense coverage.; Since crops mainly covered the tablelands for both periods, the k values were quantified under conventional tillage conditions. Thus the k values can be quantified (Table 4) using values reported in the literature, such as Haan et al. (1994), Smith and Maidment (1995), McCuen (1998) and Fernandez et al. (2003).

The watershed-specific parameter μ depends primarily on watershed morphological data (Fernandez et al., 2003) and remains the same between the two periods. In this study, it is estimated by Eqs. (14)–(16) for the baseline period, in which the SDR value in Eq. (14) is acquired from Eq. (12), based on the measured sediment yield and estimated soil erosion in the baseline period.

2.4. Estimation of contributions of influencing factors to changes in sediment load

Generally speaking, the changes in sediment load were contributed by the effects of changes in rainfall erosivity and anthropogenic activities on three processes: soil erosion processes, sediment transport processes on slopes, and sediment transport processes in stream networks.

Soil erosion is determined by the combined effects of many factors in RUSLE. The soil erodibility factor (K) in RUSLE can be considered the same between the baseline and response periods. For the L and S factors, the landscape may change due to head cut advances, bed incision and sidewall expansion of the gullies under extreme rainfall events; e.g., one measured gully showed a headcut retreat distance of 45.2 m, a bed incision depth of 5.6 m, and a sidewall expansion width of 11.7 mm during a single rainstorm occurring on July 2, 2006 (Chen et al., 2009a; Chen et al., 2009b). Thus, in order to explore the effects of extreme rainfall events on landscape change and possible LS changes, the sediment yield for each rainfall event from 1981 to 2016 was ranked (Fig. 4). It can be seen that the number of rainfall events as extreme as the one that occurred on July 2, 2006 was extremely limited across the study periods, and only occurred once in the response period, thus no significant landscape changes are thought to have occurred due to extreme rainfall in either of the two periods. Therefore, this study assumed that changes to L and S were the same for each period.

The rainfall erosivity factor (R) may have differed between the baseline and response periods due to natural changes in rainfall; the cover management factor (C) between the two periods may be different due to the various vegetation restoration projects; and the soil conservation practice factor (P) may have also changed due to terraced farmlands being introduced to the area by the government project, "Converting farmland to forest and grassland". These points suggest that the sediment load between the two periods may change due to the changes in the magnitude of soil erosion, which in turn is caused by changes in the natural factor (R) and human activities (C and P).

Sediment transported from hill slope to stream network may also change as SDR changes, since in the SEDD model, vegetation cover of forest, shrub land and grassland probably differed between the two periods. Soil conservation measures in the stream networks may also contribute to the changes in sediment load, since sediment trapped by check dams may be different in the two periods, considering that the dams were mainly built during the response period. It can be concluded that sediment load changes in the transport process were mainly caused by anthropogenic activities, including vegetation restoration on slopes, and sediment retention by check dams in the stream networks. Thus, the changes in sediment load between the two periods, and the contributions of the influencing factors, can be quantified using the

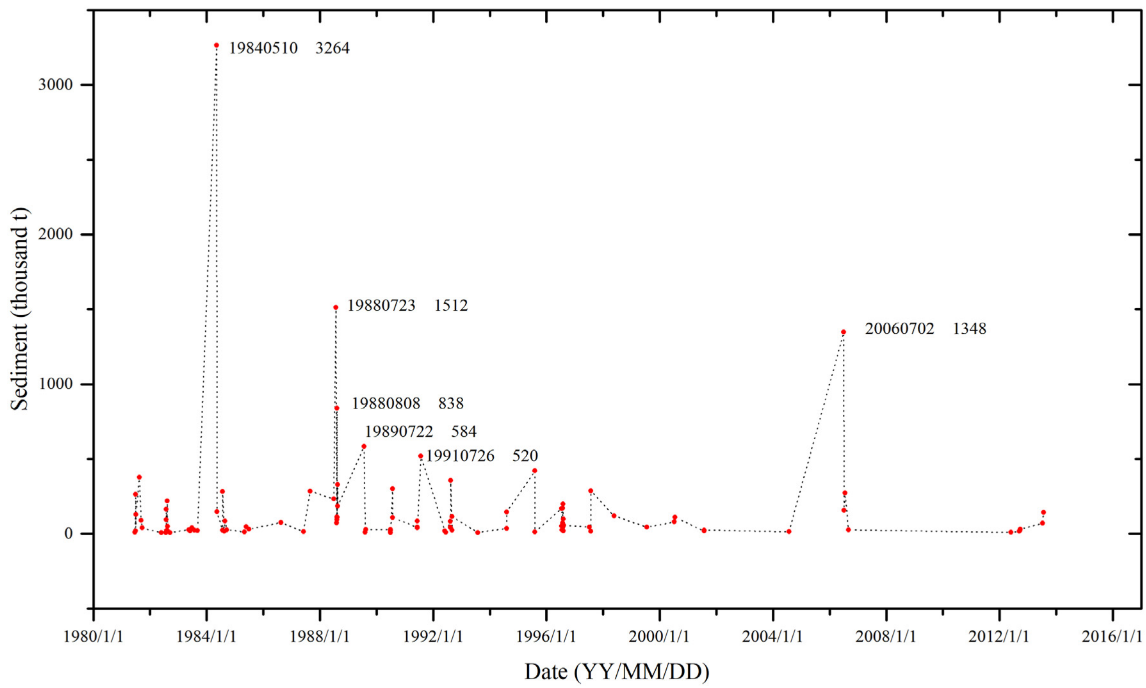

Fig. 4. Daily sediment yield for large flood events in the Yanwachuan watershed from 1981 to 2016.

following equations:

$$\Delta Y = Y_b - Y_{rm} \tag{19}$$

$$\Delta Y_A = (A_b - A_r)\, SDR_b \tag{20}$$

$$\Delta Y_{SDR} = (SDR_b - SDR_{re})A_r \tag{21}$$

$\Delta Y_C = \Delta Y - \Delta Y_A - \Delta Y_{SDR}$ (22)where, ΔY is the measured sediment change between the baseline and response periods, t; Y_{rm} is the measured sediment yield for the response period, t; and ΔY_A, ΔY_{SDR} and ΔY_C are the sediment load changes contributed by changes in soil erosion, sediment delivery ratios and sediment retention by check dams, respectively.

The measured sediment trapped by check dams can be used to validate the ΔY_C estimated from Eqs. (17)–(20). Trapped sediment data is presented in Table 3.

3. Results

3.1. Estimated soil erosion during the baseline and response periods

3.1.1. Estimated values of RUSLE factors in the Yanwachuan watershed

Mean annual rainfall erosivity from 1981 to 2016 in the Yanwachuan watershed is presented in Fig. 5. Although an obvious inter-annual variation can be observed, no significant trend was detected for inter-annual rainfall erosivity. The average rainfall erosivity in the baseline and response periods were 1383 and 1422 MJ·mm·hm^{-2}·h^{-1}·a^{-1}, respectively, showing a percentage increase of only 2.83% in the response period. The mean rainfall for both periods was 522 and 524 mm, respectively, showing a percentage increase of only 0.8%. These results indicate that changes in both rainfall and rainfall erosivity were negligible between the two periods. Based on Eq. (3), K values for the three soils were quantified as 0.014, 0.13 and 0.008 t ha h ha^{-1} MJ^{-1} mm^{-1}. The L value ranged from 0 to 14.27, with a mean value of 1.58, and the S value ranged from 0 to 9.99, with a mean value of 4.10.

The C values of forest and grasslands were estimated based on Eqs. (9)–(11). The results indicated that the NDVI values on the five selected days in July and August of 1986, 1991, 2000, 2009 and 2017 (Table 2) were 0.34, 0.37, 0.33, 0.53, and 0.53, respectively. It can be seen that the NDVI values were similar up to and including the year 2000, but increased substantially in the new century, which is consistent with the introduction of soil conservation projects, which mainly began in 1994. In this study, land use data were available for the years 1990, 2000, 2010 and 2015, thus the land use data for 1990 and 2010 were chosen to represent the land use scenarios for the baseline period (1981–1994) and the response period (1995–2016), respectively. The spatial distributions of C values for forests and grasslands in both periods were

Table 4
The k values for various land use types in this study.

Period	Forests	Grasslands	Agricultural lands	Construction sites	Water bodies
Baseline	0.21	0.64	2.77	6.28	0
Response	0.43	0.46			

Table 3
Sediment trapped by check dams for different periods measured by Xifeng Station.

	Period	Average annual trapped sediment (10^4 t a^{-1})	No. of years	Average annual sediment reduction (10^4 t a^{-1})	Total sediment reduction (10^4 t a^{-1})
Baseline period	1981–1994	8.01	14	0	0
Response period	1995–1999	8.72	5	0.71	3.55
	2000–2004	18.08	5	10.07	50.36
	2008–2013	32.27	6	24.26	145.58
	1995–2004 & 2008–2013	20.47	16	12.47	199.48

Table 5
Calculated sediment reduction and the contributions of influencing factors.

	Measured sediment	Estimated soil erosion	SDR	Influencing factor	Sediment reduction	Percentage (%)
Baseline period	9.44	10.84	0.87	Erosion reduction	5.14	75.47
Response period	2.62	4.72	0.84	SDR reduction	0.14	2.08
Difference	6.81	6.12	0.03	Check dam reduction	1.53	22.45
Percentage (%)	72.19	56.44	3.45	Total reduction	6.81	100%

*The unit for measured sediment, estimated soil erosion and sediment reduction was 10^5 t a^{-1}.

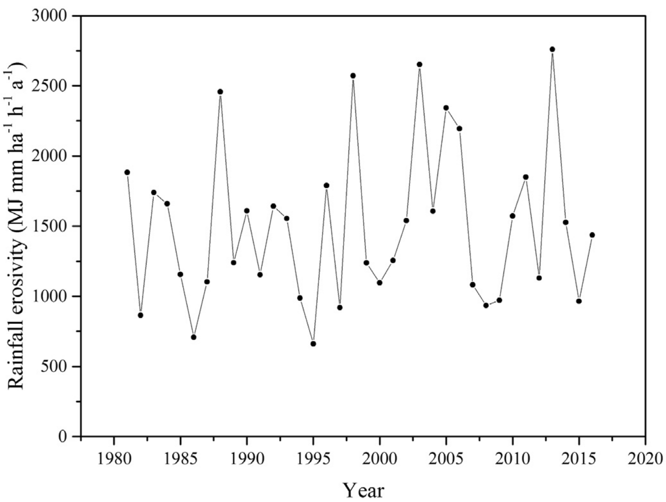

Fig. 5. Annual rainfall erosivity in the Yanwachuan watershed from 1981 to 2016.

estimated using the NDVI values calculated for 1991 and 2009, and the land use data in 1990 and 2010. The mean C values of forests in the baseline and response period were 0.18 and 0.05, and the C values of grassland were 0.24 and 0.07, respectively. This represents a substantial reduction in C values for both forests and grassland between the two periods, probably due to ecological restoration that formed part of the soil conservation projects, such as the “Converting slope farmland to forest” Project.

The C values of agricultural lands, construction sites and water bodies were quantified as previously indicated, thus the spatial distribution of C values for all the land use types in both periods could be reconstructed (Fig. 6). The results showed a mean C value of 0.253 in the baseline period, 2.01 times high than the mean C value of 0.126 calculated for the response period, indicating substantial changes between the two periods.

Mean *P* values for the baseline and response periods were calculated to be 0.8473 and 0.8466, respectively, indicating changes in P were negligible over the studied period. This was probably because the proportion of agricultural lands on slopes was very low (1.8%), with agricultural lands mainly being situated on the vast tablelands.

3.1.2. Estimated soil erosion in the baseline and response periods

The spatial distribution of soil erosion in the Yanwachuan watershed for both periods can be quantified using Eq. (1). For the control area of the Yanwachuan hydrometric station, soil erosion rates in the baseline and response periods were 2054.3 and 1451.5 t km^{-2} a^{-1}, and the total soil erosion was 6.69×10^5 and 4.72×10^5 t a^{-1}, respectively. However, the measured sediment yields at Yanwachuan hydrological station in the baseline and response periods were 9.44×10^5 and 2.62×10^5 t a^{-1}, respectively. It can be seen that the estimated soil erosion in the baseline period was substantially lower than the measured sediment yield, implying that the estimated soil erosion may not reflect the actual soil erosion.

Measured sediment yields in 1984 and 1988 were 3.96×10^6 t and 3.56×10^6 t (Fig. 2), respectively, which is not only notably higher than the measured sediment yields for the others years in the baseline period, but also substantially higher than the estimated soil erosion. These two large sediment yields were primarily caused by high-intensity extreme rainfall events on May 10–14, 1984 and July 22, 1988. The rainstorm center of the torrential rain that occurred on July 22, 1988 was on the tableland (Fig. 7), with about 70–80 km^2 of tableland contributing to the generation of the excessive runoff. The rainstorm resulted in 3.75×10^6 m^3 of runoff, accounting for 61% of the total daily flow discharge (66.4 m^3 s^{-1}, resulting in 5.74×10^6 m^3 for the day). The effect of these two extreme rainfall events on soil erosion was not fully predicted by RUSLE, which is probably due to the unique characteristics of soil erosion in the tableland and gully region. In RUSLE, rainfall erosivity is designed to represent the erosive energy of rainfall and runoff; however, the estimated R values in 1984 and 1988 show that the destructive power of excessive rainfall is not fully reflected by the R factor, since they are similar to other years. This is probably because in RUSLE both runoff and sediment are generated on slope land while in the Yanwachuan watershed, the large amount of runoff generated on May 10–14, 1984 and July 23, 1988 came from the tablelands. This implies that the RUSLE model cannot fully predict soil erosion in tableland and gully regions, especially when extreme rainfall events have occurred.

Since the extreme rainfall events in 1984 and 1988 were both high-intensity and low-duration, and the hyper-concentrated sediment load flowed rapidly to the river networks, the measured sediment at the Yanwachuan hydrometric station can be approximately represent total soil erosion. Many previous studies in the Loess Plateau have indicated that the sediment delivery ratios in small or medium scale watersheds during torrential rains are close to 1 (Gong and Xiong, 1979; Mou and Meng, 1982; Cao et al., 1993). Thus, the total soil erosion in the baseline period can be revised using the following equation:

$$A_b = (12A_{bu} + Y_{1984} + Y_{1988})/14 \tag{23}$$

where, A_{bu} is the estimated average annual soil erosion for the baseline period based on RUSLE, which was 6.69×10^5 t a^{-1}; Y_{1984} and Y_{1988} are the measured sediment yields in 1984 and 1988, which were 3.96×10^6 t and 3.56×10^6 t, respectively; 14 is the number of years the baseline period spans (1981–1994); and 12 is the total years of the baseline period with the years 1984 and 1988 removed. The estimated soil erosion in the baseline period was 10.84×10^5 t a^{-1}, 2.30 times higher than the soil erosion estimated 4.72×10^5 t a^{-1} in the response period, indicating that soil erosion decreased substantially from the baseline period to the response period. According to Eq. (12), the estimated SDR was 0.87 in the baseline period, similar to values recorded in the Loess Plateau e.g., 0.91 in Beiluohe watershed (Jing, 1999), 0.90 in Malianhe watershed (Jing, 1999), and 0.83 in Dalihe watershed (Mou and Meng, 1982).

3.2. Estimated sediment yield in the response period

The SDR value in the baseline period was calculated as 0.87 using Eq. (12), then Eqs. (14)–(16) were used to calculate a value of 3.80 for the watershed-specific parameter, μ. Following this, the spatial distributions of SDR in both periods were calculated using Eqs. (14)–(16). The mean SDR value in the response period was calculated to be 0.84,

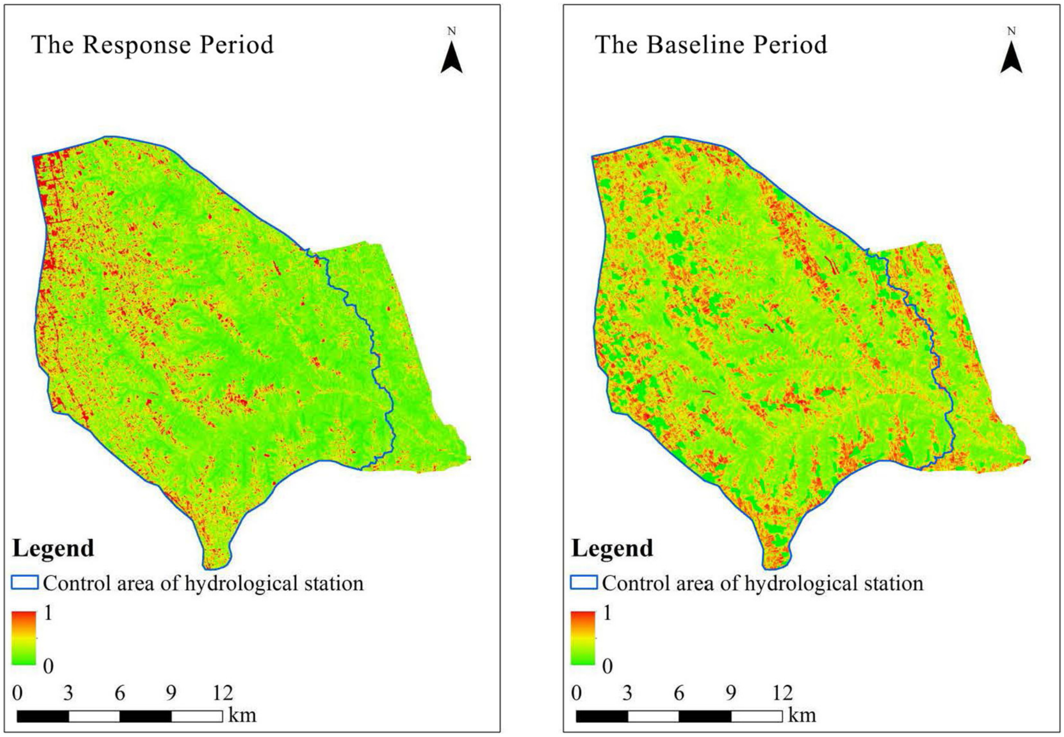

Fig. 6. C values of the baseline and response periods in the Yanwachuan watershed.

3.45% lower than the mean SDR value calculated for the baseline period. Estimated sediment entering the stream networks in the response period was quantified by multiplying estimated soil erosion and sediment delivery ratio in the ArcGIS environment. Finally, the estimated average annual sediment yields into the stream networks were quantified to be 3.97×10^5 t a^{-1}.

3.3. Contributions of influencing factors to changes in sediment load

Values for measured sediment yield, estimated soil erosion and SDRs calculated using Eqs. (17–20) are presented in Table 5. The values show that changes in soil erosion, SDR and sediment retention by check dams have contributed 75.47, 2.08 and 22.45% of the total sediment reduction, respectively.

As previously stated, the change in soil erosion between the two periods is caused by both natural factors (R) and anthropogenic activities (C and P). The changes in values of R, C and P factors have been analyzed, and the results indicate that, compared with the baseline period, rainfall and rainfall erosivity (R) only increased 0.8% and 2.8%, respectively. This indicates that the effects of climatic changes on changes in soil erosion and sediment load were very small. The differences in calculated P factor for the two periods were also negligible. However, the C values changed substantially, from 0.253 in the baseline period, to 0.126 in the response period, indicating that changes in land use and vegetation cover contributed substantially to changes in soil erosion and sediment load. The change in SDRs was caused by the change in *k* values due to land use and vegetation cover changes. The sediment trapped by the check dams in the river networks also contributed to the changes in sediment load at the Yanwachuan hydrometric station, since the check dams were mainly built in the response period. It can be concluded that human-induced vegetation restoration contributed 77.55% of the sediment reduction, while the check dams contributed the other 22.45%.

3.4. Validation of the contribution of check dams to changes in sediment load

The estimated and measured average annual sediment in the response period were 3.97×10^5 t a^{-1} and 2.62×10^5 t a^{-1}, respectively. It can be inferred that the difference, 1.35×10^5 t a^{-1} was trapped by check dams in the stream networks. In Table 5, the estimated sediment trapped by check dams was 1.53×10^5 t a^{-1}, 13.8% higher than the inferred value, indicating that the results in this study are reasonable.

The measured sediment trapped by check dams for 1995–2004 and 2008–2013 is presented in Table 3, and can be compared to the estimated values. The total measured sediment trapped by the check dams for 1995–2004 and 2008–2013 was 199.48×10^4 t (Table 3), resulting in an average annual value of 1.25×10^5 t a^{-1}, 18.44% lower than the estimated 1.53×10^5 t a^{-1}, indicating that the results in this study are reasonable.

4. Discussion

In this study, the changes in sediment load and their influencing factors for a typical watershed in the tableland and gully region in the Loess Plateau, China, was analyzed by the combined use of the RUSLE and SEDD models. Lots of measured data, such as rainfall, flow discharge, sediment load, and sediment trapped by the check dams, and the parameters in both models are used for estimation and analysis, meaning considerable errors can be accumulated if the measured or estimated values of the parameters are not reliable. Accurate measurements of hydrometric data and sediment trapped by check dams are difficult, especially during large floods. In the Yanwachuan watershed, hyper-concentrated flows are essentially uniform flows with a high suspended fine-material concentration (Rickenmann, 1991). According to data from several hydrometric stations, the vertical distribution and the cross-sectional distribution of sediment concentration in the hyper-concentrated flow are uniform (Zhao and Niu, 1983; Li, 2005), thus, the measured sediment yield measured during large floods can be

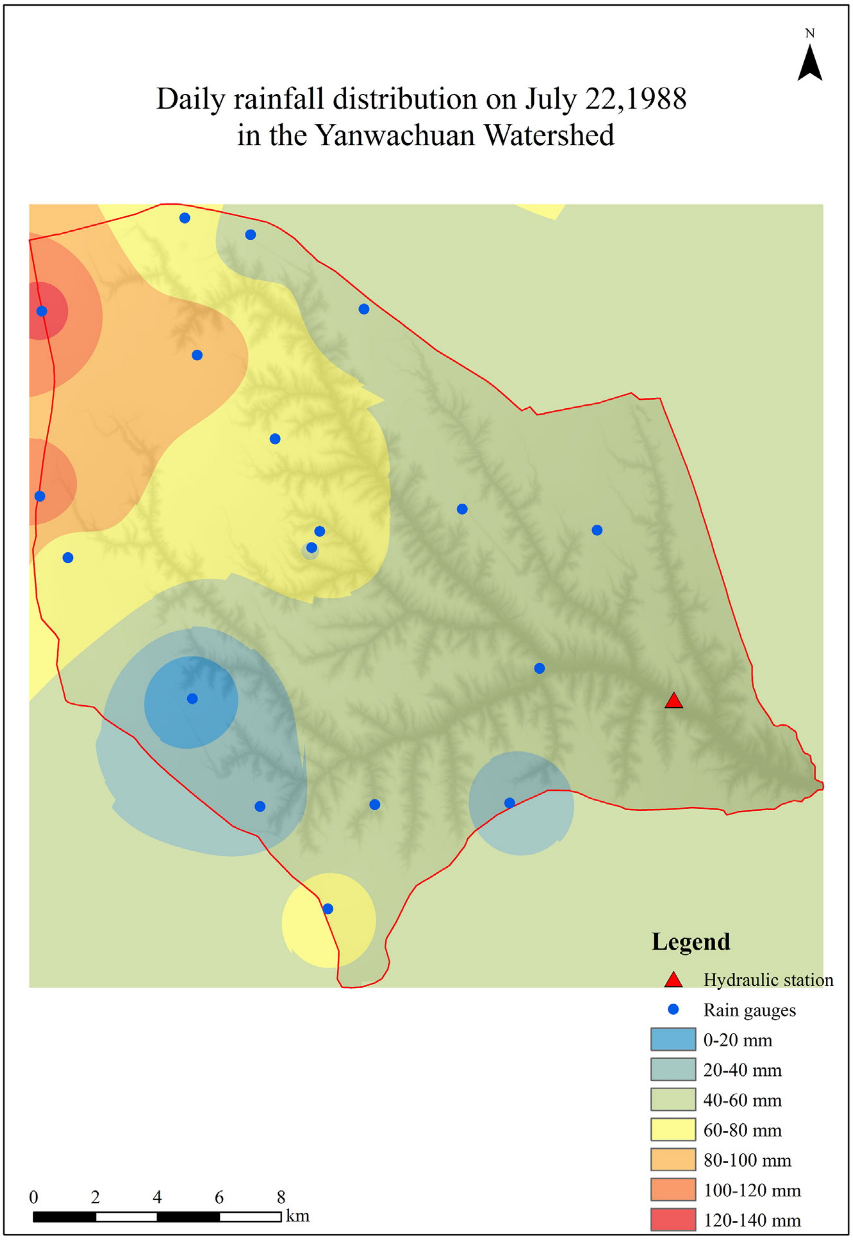

Fig. 7. Spatial distribution of the extreme rainfall event that occurred on July 22, 1988.

considered reliable. Despite that, more experimental studies on sediment measurement should be conducted to better represent the sediment concentration characteristics during flood events, which are of great significance for soil erosion studies in the tableland and gully region of the Loess Plateau. Similar questions also arise for the measurement of sediment trapped by check dams. In this study, a method applied to large numbers of check dams in small or medium watersheds across the Loess Plateau was used to estimate sediment retention by measuring sediment height before or after flood events or rainy seasons. This is an effective method considering the large number of check dams in the same watershed; however, comparisons between results gathered using this method and results gathered by new techniques should be made, to improve the accuracy of the method. These tests should be conducted in the near future in the Yanwachuan watershed, since check dams play a more important role in reducing the sediment load to the rivers. For the RUSLE analysis, rainfall erosivity was estimated based on daily rainfall data, due to the lack of high-resolution rainfall data in the earlier years of the study period. This method of estimation leads to errors in annual R values that are reported at < 11% (Zhang et al., 2003; Xie et al., 2016). Despite this degree of error being acceptable in the current study, caution must be used when estimating the event-based rainfall erosivity, especially for extreme rainfall events, since the daily data does not reflect rainfall intensity and during these events, which are important for runoff accumulation on the tableland. High-resolution rainfall data is now being measured in the Yanwachuan watershed, facilitating more accurate rainfall erosivity estimations in the near future, which will be valuable for accurately estimating soil loss. For the SEDD model, the *k* values were rigorously quantified based on published values for the various land use types (Haan et al., 1994; Smith and Maidment, 1995; McCuen, 1998; Fernandez et al., 2003); however, these values have not been validated in the local regions, and thus may carry some error. It can be seen that the accuracy of measured data and the parameters in the models are important to the estimation process and can greatly affect the reliability of the results, thus more work should be conducted to ensure the accuracy of the basic data and to improve the performance of the models.

The results of this study indicated that the sediment load in the Yanwachuan watershed, in the tableland and gully region in the Loess Plateau, decreased substantially in the response period, which is consistent with the majority of similar studies conducted in the Loess Plateau (Table 1). The MK mutation test has been conducted in many studies, and the reported year of mutation was similar between various studies, such as 1997 in the Yanhe watershed (Ren et al., 2012), 1990 in Huangfuchuan watershed (Zhao et al., 2017), and 1999 in the Loess Plateau (Wang et al., 2015a). These dates are all consistent with the year 1994 calculated in this study, implying that soil conservation measures were implemented at the same period throughout the Loess Plateau. It can be also seen that the main factors influencing changes in sediment load were also similar throughout the Loess Plateau, mainly consisting of vegetation restoration, check dam retention and terraces in the slope farmland, despite the quantitative effects differing substantially in different studies (Table 1). Moreover, these studies were all conducted in the hill and gully region, while studies in other regions such as the tableland and gully region are scarce. Thus, more studies on changes in sediment load of the watersheds in the Loess Plateau should be planned and undertaken, to increase the reliability of results, and thereby provide valuable guidance for soil conservation strategy in the Loess Plateau.

In this study, in the tableland and gully region of the Loess Plateau, severe soil erosion was usually caused by extreme rainfall events. This has been widely reported in other studies (Zhu, 1954; Yang et al., 1989; Xing et al., 1991; Li et al., 1993; Xue, 1995; Wang et al., 2005; Tian et al., 2008; Zhang et al., 2015a, 2015b). Zhu (1954) noticed that soil erosion was very slight under ordinary rainfall conditions, whereas huge soil erosion was caused by extreme rainfall conditions, due to the large amount of runoff generated on the tablelands flowing into nearby gullies. This was verified by long-term field measurements in the nearby Nanxiaohegou watershed (Fig. 1): soil erosion was usually slight except under exceptional rainfall conditions (*Xifeng experimental station of soil and water conservation and bureau of water and electric in Qingyang*, 1974). Li et al. (1993) pointed out that the large amount of runoff generated by excessive rainfall on the vast tablelands would cause severe damage because the great amount of runoff flows from the high tablelands to the deep valleys very rapidly. Such rapid flows usually have the destructive power to detach slope soils and transport them into the valleys, resulting in extreme soil erosion, and the potential to cause natural disasters (Xing et al., 1991; Tian et al., 2008). However, the relationships between rainfall characteristics and excessive runoff for extreme rainfall events still remain unclear. The coupled effects of extreme rainfall characteristics and the local terrain form a bottleneck in soil erosion research and soil conservation management with respect to the tableland and gully region: despite the importance of extreme rainfall events on soil erosion being widely known, details of the quantitative relationship between extreme rainfall events and soil erosion are still lacking. It can be concluded from this study that rainfall erosivity estimated from the daily rainfall data cannot fully predict the destructive power of the excessive runoff generated on the tableland during extreme rainfall events; thus, such estimations will substantially underestimate the soil loss under extreme rainfall events. Studies on the relationships between extreme rainfall and the excessive runoff generated on the tableland, and the relationships between extreme rainfall and sediment yield, should be carried out in the near future, and a new parameter which can represent the excessive runoff generated on the tableland should be established. This would help to reveal the soil erosion mechanism under the extreme rainfall events, and clarify the unique characteristics of the tableland and gully region.

The results of this study showed that the mean contribution of check dams to changes in sediment load was about 22.5%, indicating that check dams played an important role in sediment reduction. According to Table 3, sediment trapped by the check dams increased year on year, and the annual average trapped sediment for 2008–2013 was 3.23×10^5 t a^{-1}. Meanwhile, annual soil erosion decreased substantially, and the annual average soil erosion for 1995–2016 was 4.72×10^5 t a^{-1}, indicating that check dams trapped 68.13% of eroded soil throughout 2008–2013. This implies that, currently, the contribution of check dams to sediment reduction is higher than the contribution of vegetation cover, which was in accordance with the fact that many check dams have been built since 1990s. Vegetation cover of forest and grassland reached 77.0% and 67.7%, respectively, in 2009. Thus, it is unlikely that vegetation cover will increase by a great deal, so the contribution of vegetation cover to sediment reduction also is likely to remain stable. In turn, this implies that the effect of check dams on sediment reduction may continue to increase in the future. It is expected that the storage capacity of these dams will decrease sharply, which will shorten their designed lifespan. Zhao et al. (2017) noted risks associated with check dams being filled rapidly in the Huangfuchuan watershed; besides large floods carrying sediment into the check dams, they can also damage or destroy the dams and release the stored sediment. Examples include the large floods in 1978 in the Chabagou watershed (Zhang et al., 2010), and the floods in 2015 in the Wudinghe River Basin. Liu et al. (2017) reported that for the Loess Plateau, 25.2% of the 5658 total key dams, and 44.5% of the 11,248 total medium-sized dams, are likely to lose the ability to block sand, while the sediment-retaining ability of other dams will continue to decrease. Under this circumstance, the check dams in the Yanwachuan watershed must be protected, and further studies on effective measures for protecting check dams should be carried out, to ensure maximum efficiency of check dams on sediment reduction.

5. Conclusions

1) Sediment load of the Yanwachuan watershed in the table land and gully region of the Loess Plateau decreased substantially for the period of 1981–2016, with 1994 being identified as the year of mutation;
2) Change in sediment load was mainly influenced by human induced vegetation restoration across the watershed and check dams in the stream networks, which accounted for about 77.55% and 22.45% of the sediment load reduction, respectively, while the effects of climatic change and terraced farmland were negligible;
3) The effect of check dams on sediment retention is likely to increase in the future, thus effective measures should be implemented to protect check dams, and further studies should be performed to ensure the effects of check dams on sediment reduction are maximized.

Acknowledgements

This study was funded by the National Natural Science Foundation of China (No. 41877073), the Young Elite Scientist Sponsorship Program by the China Association for Science and Technology (2015–2017), the IWHR Research & Development Support Program (SE0145C202017).

References

Ai, S.Z., Hao, F.B., Ma, S.B., Ma, S.P., 2005. Application of GPS in sediment monitoring of silt retention dams. China Water Resources 12, 54–56 (In Chinese with English Abstract).
Amore, E., Modica, C., Nearing, M.A., Santoro, V.C., 2004. Scale effect in USLE and WEPP application for soil erosion computation from three Sicilian basins. J. Hydrol. 293 (1), 100–114.
Cao, W.H., Zhang, Q.S., Jiang, N.S., 1993. The study on mathematical model for sediment yields caused by one storm in Loess zone. J. Sediment. Res. 3 (1), 1–13 (in Chinese with English Abstract).
Carriquiry, J.D., Sanchez, A., 1999. Sedimentation in the Colorado river delta and upper gulf of California after nearly a century of discharge loss. Mar. Geol. 158, 125–145.
Chen, H., 2000. Effect of rainfall runoff on sediment delivery ratio of Daili basin system. J. Soil Water Conserv. 14 (5), 19–26 (in Chinese with English Abstract).
Chen, Z.Y., Li, J.F., Shen, H.T., Wang, Z.H., 2001. Yangtze River of China: historical analysis of discharge variability and sediment flux. Geomorphology 41, 77–91.

Chen, X., Zhang, E., Mu, H., Zong, Y., 2005. A preliminary analysis of human impacts on sediment discharges from the Yangtze, China, into the sea. J. Coast. Res. 21, 515–521.

Chen, X.Q., Yan, Y., Fu, R.S., Dou, X., Zhang, E.F., 2008. Sediment transport from the Yangtze River, China, into the sea over the Post-Three Gorge Dam Period: a discussion. Quat. Int. 186, 55–64.

Chen, S.Y., Xu, J.M., Wang, W.L., 2009a. The research on erosional types and process of head-cut on Dongzhiyuan of Loess Plateau. Chin. Agri. Sci. Bull. 25 (9), 258–263 (in Chinese with English Abstract).

Chen, S.Y., Xu, J.M., Wang, W.L., Zhao, A.C., Li, H.Y., 2009b. Erosion features of head-cut and its control measures on Dongzhiyuan of the loess plateau. Bull. Soil Water Conserv. 29 (4), 37–41 (in Chinese with English Abstract).

Cho, H.L., Jeoung, J.C., 2005. Estimating soil loss in alpine farmland with RUSLE and SEDD. Journal of Korea Spatial Information Society 13 (1), 79–90.

Dai, S.B., Lu, X.X., 2014. Sediment load change in the Yangtze River (Changjiang): a review. Geomorphology 215 (12), 60–73.

Dai, S.B., Yang, S.L., Cai, A.M., Lu, X.X., 2008. A preliminary estimate of human and natural contributions to the decline in sediment flux from the Yangtze River to the East China Sea. Quat. Int. 186 (1), 43–54.

Deng, M.J., Wang, Z.J., Wang, J.Y., 2011. Analysis of Balkhash Lake ecological water level evolvement and its regulation strategy. Hydrological Engineering 42 (4), 403–413.

Desmet, P.J.J., Govers, G., 1996. A GIS procedure for automatically calculating the USLE LS factor on topographically complex landscape units. J. Soil Water Conserv. 51 (5), 427–433.

Dong, A.X., 2005. Historical Records of Meteorological Disasters in China: Gansu Province. China Meteorological Press, Beijing (in Chinese).

Fernandez, C., Wu, J.Q., McCool, D.K., Stockle, C.O., 2003. Estimating water erosion and sediment yield with GIS, RUSLE and SEDD. J. Soil Water Conserv. 58 (3), 128–136.

Ferro, V., Porto, P., 2000. Sediment delivery distributed model (SEDD). J. Hydrol. Eng. 5 (4), 411–422.

Fu, G., Chen, S., McCool, D.K., 2006. Modelling the impacts of no-till practice on soil erosion and sediment yield with RUSLE, SEDD, and Arcview GIS. Soil &Tillage Research 85 (1–2), 38–49.

Fu, S.H., Liu, B.Y., Zhou, G.Y., Sun, Z.X., Zhu, X.L., 2015. Calculation tool of topographic factors. Science of Soil and Water Conservation 13 (5), 105–110 (in Chinese with English Abstract).

Gabriels, D., Ghekiere, G., Schiettecatte, W., Rottiers, I., 2003. Assessment of USLE cover-management C factors for 40 crops rotation systems on arable farms in the Kemmelbeek watershed, Belgium. Soil &Tillage Research 74 (1), 47–53.

Gao, P., Mu, X.M., Li, R., Wang, W., 2009. Analyses on trend and driving force of runoff and sediment load in the Wuding River. Journal of Sediment Research 10 (5), 22–28 (in Chinese with English Abstract).

Gao, P., Mu, X.M., Wang, F., Li, R., 2011. Changes in stream flow and sediment discharge and the response to human activities in the middle reaches of the Yellow River. Hydrol. Earth Syst. Sci. 15, 1–10.

Gao, H.D., Li, Z.B., Li, P., Jia, L.L., Xu, G.C., Ren, Z.P., Pang, G.W., Zhao, B.H., 2015. The capacity of soil loss control in the Loess Plateau based on soil erosion control degree. Acta Geograph. Sin. 70 (9), 1503–1515 (in Chinese with English Abstract).

Geng, C., 2011. Soil Erosion of Small Watershed Study by GIS Technology. Master Dissertation. Xi'an: Xi'an University of Science and Technology (in Chinese with English Abstract).

Gong, S.Y., Xiong, G.S., 1979. The source and geographical distribution of sediment in Yellow River. Yellow River 1, 9–20 (in Chinese).

Haan, C.T., Barfield, B.J., Hayes, J.C., 1994. Design Hydrology and Sedimentology for Small Catchments. vol. 588 Academic Press.

Hessel, R., 2006. Consequences of hyper-concentrated flow for process-based soil erosion modelling on the Chinese Loess Plateau. Earth Surfaces Processes and Landforms 31, 1100–1114.

Jain, M.K., Kothyari, U.C., 2000. Estimation of soil erosion and sediment yield using GIS. Hydrol. Sci. J. 45 (5), 771–786.

Jiang, Z.S., Wang, Z.Q., Liu, Z., 1996. Quantitative study on spatial variation of soil erosion in a small watershed in the Loess Hilly Region. Journal of Soil Erosion and Soil Conservation 2 (1), 1–9 (in Chinese with English Abstract).

Jing, K., 1999. Sediment transport in Jinghe River and Beiluo River. Yellow River 21 (12), 8–19 (in Chinese).

Kamaludin, H., Lihan, T., Rahman, Z.A., Mustapha, M.A., Idris, W.M.R., Rahim, S.A., 2013. Integration of remote sensing, RUSLE and GIS to model potential soil loss and sediment yield. Hydrol. Earth Syst. Sci. 10, 4567–4596.

Kinnell, P.I.A., 2000. AGNPS-UM: applying the USLE-M within the agricultural non-point source pollution model. Environ. Model Softw. 15 (3), 331–341.

Li, W.Q., 2005. Characteristics of sediment concentration for hyper-concentrated flow and advices for the improvement of sediment concentration measurement. Soil and Water Conservation Science and Technology in Shanxi 6 (2), 21–22 (in Chinese).

Li, D., He, Z.F., Wang, X.H., Yang, H.M., 1993. The benefits of retaining water and sediment in the comprehensive harnessment of Xiaohegou watershed. Yellow River 7, 22–25 (in Chinese with English Abstract).

Li, P.F., Mu, X.M., Holden, J., Wu, Y.P., Irvine, B., Wang, F., Gao, P., Zhao, G.J., Sun, W.Y., 2017. Comparison of soil erosion models used to study the Chinese Loess Plateau. Earth Sci. Rev. 170, 17–30.

Liu, X.Y., He, D.Y., 2013. Temporal and spatial distribution and its change trend of suspended sediment transport in the Nujiang River Basin. Acta Geograph. Sin. 68 (3), 365–371.

Liu, B.Y., Nearing, M.A., Risse, L.M., 1994. Slope gradient effects on soil loss for steep slope. Transactions of the ASAE 37 (6), 1835–1840.

Liu, C., Wang, Z.Y., Sui, J.Y., 2007. Analysis on variation of seagoing water and sediment load in main rivers of China. J. Hydrol. Eng. 38 (12), 1444–1452.

Liu, C., Wang, J.J., He, Y., 2013. Change in sediment loads in the Lancang-Mekong River and its influencing factors. Advances in Science and Technology of Water Resources 33 (1), 7–12.

Liu, X.Y., Gao, Y.F., Wang, F.G., 2017. Quantity and distribution of warping dams that still have sediment retaining ability in the Loess Plateau. Yellow River 39 (4), 1–6 (in Chinese with English Abstract).

McCool, D.K., Brown, L.C., Foster, G.R., Mutchler, C.K., Meyer, L.D., 1989. Revised slope length factor for the Universal Soil Loss Equation. Transactions of the ASAE 30 (5), 1387–1396.

McCuen, R.H., 1998. Hydrologic Analysis and Design. Prentice-Hall, New Jersey.

Mellerowicz, K.T., Rees, H.W., Chow, T.L., Ghanem, I., 1994. Soil conservation planning at the watershed level using the Universal Soil Loss Equation with GIS and microcomputer technologies: a case study. J. Soil Water Conserv. 49 (2), 194–200.

Merriam, C.F., 1937. A comprehensive study of rainfall on the Susquehanna Valley. Transactions of the American Geophysics Union 18, 471–476.

Merritt, W.S., Letcher, R.A., Jakeman, A.J., 2003. A review of erosion and sediment transport models. Environ. Model Softw. 18 (8), 761–799.

Meybeck, M., 1988. How to establish and use world budgets of river material. In: Lerman, A., Meybeck, A. (Eds.), Physical and Chemical Weathering in Geochemical Cycles. Kluwer Academic Publishing, Dordrecht, the Netherlands, pp. 247–272.

Miao, C.Y., Ni, J.R., Borthwick, A.G.L., Yang, L., 2011. A preliminary estimate of human and natural contributions to the changes in water discharge and sediment load in the Yellow River. Glob. Planet. Chang. 76, 196–205.

Montgomery, D.R., 2007. Soil erosion and agricultural sustainability. Proc. Natl. Acad. Sci. U. S. A. 104, 13268–13272.

Mou, J.Z., Meng, Q.M., 1982. A study on sediment delivery ratio for estimating watershed sediment yield. Journal of Sediment Research 6 (2), 60–65 (in Chinese).

Mu, X.M., Zhang, X.Q., Gao, P., Wang, F., 2010. Theory of double mass curves and its applications in hydrology and meteorology. Journal of China Hydrology 30 (4), 47–51 (in Chinese with English Abstract).

Perrin C, Michel C, Andréassian V, 2001. Does a large number of parameters enhance model performance? Comparative assessment of common catchment model structures on 429 catchments. J. Hydrol., 242 (3–4): 275–301.

Ren, Z.P., Zhang, G.H., Yang, Q.K., 2012. Characteristics of runoff and sediment variation in Yanhe River basin in last 50 years. Journal of China Hydrology 32 (5), 81–86 (in Chinese with English Abstract).

Renard, K.G., Foster, G.A., Weesies, D.K., McCool Yoder, D.C., 1997. Predicting soil erosion by water: A guide to conservation planning with the revised universal soil loss equation (RUSLE). In: Agricultural Handbook no.537. United States Department of Agriculture, Washington DC.

Rickenmann, D., 1991. Hyper-concentrated flow and sediment transport at steep slopes. J. Hydraul. Eng. 117 (11), 1419–1439.

Rustomji, P., Zhang, X.P., Hairsine, P.B., Zhang, L., Zhao, J., 2008. River sediment load and concentration response to changes in hydrology and catchment management in the Loess Plateau region of China. Water Resour. Res. 44 (7), 148–152.

Smith PNH, Maidment DR, 1995. Hydrologic data development system. CRWR Online Report No.95-1. Center for Research in Water Resources, University of Texas, Austin, TX.

Soil inventory office in Qingyang, 1989. Soils in Qingyang, Gansu Province. Gansu Science & Technology Press, Lanzhou (in Chinese).

Syvitski, J.P.M., Vörösmarty, C.J., Kettner, A.J., Green, P., 2005. Impact of humans on the flux of terrestrial sediment to the global coastal ocean. Science 308 (5720), 376–380.

Taguas, E.V., Moral, C., Ayuso, J.L., Perez, R., Gomez, J.A., 2011. Modeling the spatial distribution of water erosion within a Spanish olive orchard micro-catchment using the SEDD model. Geomorphology 133 (1–2), 47–56.

Tian, X.F., Jia, Z.X., Liu, B., Wang, H.B., Wu, Y.H., Gong, C.W., 2008. A Study on the Soil Erosion Processes and the Effects of Soil Conservation Measures in a Typical Small Watershed in the Tableland and Gully Region in the Loess Plateau. the Yellow River Water Conservancy Press, Zhengzhou (in Chinese).

United States Department of Agriculture, 1990. EPIC-Erosion/Productivity Impact Calculator 1. Model Documentation. Technical Bulletin Number 1768. USDA-ARS, Washington D. C.

USDA Soil Conservation Service, 1975. Urban hydrology for small watersheds. Technical Release No.55. Washington DC.

Vörösmarty, C.J., Meybeck, M., Fekete, B., Sharma, K., Green, P., Syvitski, J.P.M., 2003. Anthropogenic sediment retention: major global impact from registered river impoundments. Glob. Planet. Chang. 39 (1–2), 169–190.

Wainwright, J., Mulligan, M., 2013. Environmental Modeling: Finding Simplicity in Complexity. Wiley-Blackwell Publishing Ltd, Chichester.

Walling, D.E., Fang, D., 2003. Recent trends in the suspended sediment loads of the world's rivers. Glob. Planet. Chang. 39, 111–126.

Wang, W.T., Li, J.P., Zhang, T.F., Huang, B., Ren, J.B., 2005. Exceptionally early heavy rain case study in Eastern Gansu Province. Meteorological Science and Technology 33 (4), 330–333 (in Chinese with English Abstract).

Wang, F., Mu, X.M., Jiao, J.Y., Li, R., 2007a. Impact of human activities on runoff and sediment change of Yanhe River based on the periods divided by sediment concentration. Journal of Sediment Research 4, 8–13 (in Chinese with English Abstract).

Wang, H.J., Yang, Z.S., Saito, Y., Liu, J.P., Sun, X.X., Wang, Y., 2007b. Stepwise decreased of the Huanghe (Yellow River) sediment load (1950-2005): impacts of climatic change and human activities. Glob. Planet. Chang. 57, 331–354.

Wang, S., Fu, B.J., Piao, S.L., Lv, Y.H., Ciais, P., Feng, X.M., Wang, Y.F., 2015a. Reduced sediment transport in the Yellow River due to anthropogenic changes. Nat. Geosci. 9 (1), 38–41.

Wang, Y., Liu, W.Z., Li, H.Y., Zhang, X.P., 2015b. The flow-sediment relationship and its response to watershed management in Yanwachuan watershed, Loess Plateau Gully

Region, China. Journal of Natural Resources 30 (8), 1403–1413 (in Chinese with English Abstract).
Wen, A.B., Liu, S.Z., Fan, J.R., Zhu, P.Y., 2002. Current change on sedimentation and control its method in middle Yalungtsangpo River. J. Soil Water Conserv. 16 (6), 148–150.
Williams, J.R., Berndt, H.D., 1977. Sediment yield prediction based on watershed hydrology. Transactions of the ASAE 20 (6), 1100–1104.
Wilson, J.P., 1986. Estimating the topographic factor in the universal soil loss equation for watersheds. J. Soil Water Conserv. 41 (3), 179–184.
Wischmeier, W.H., Johnson, C.B., Gross, B.V., 1971. A soil erodibility nomograph for farmland and construction site. J. Soil Water Conserv. 26, 189–193.
Xie, Y., Yin, S.Q., Liu, B.Y., Nearing, M.A., Zhao, Y., 2016. Models for estimating daily rainfall erosivity in China. J. Hydrol. 535, 547–558.
Xifeng experimental station of soil and water conservation and bureau of water and electric in Qingyang. In: Horizontal Strip Field in the Table Lands. Water Resources and Electric Power Press, Beijing (in Chinese).
Xing, T.Y., Li, Z., Liu, P.L., Jia, X.A., Liu, Y., 1991. Survey and evaluation of disaster caused by heavy rainstorm occurred on July 23, 1988 and water and soil conservation measured in Xifeng area, Gansu Province. Bulletin of Soil and Water Conservation 11 (3), 40–47 (in Chinese with English Abstract).
Xu, J.X., 2004. Response of erosion and sediment producing processes to soil and water conservation measures in the Wudinghe River Basin. Acta Geograph. Sin. 59 (6), 972–981 (in Chinese with English Abstract).
Xu, J.X., 2010. Effect of artificial sediment sinks on sediment delivery ratio: an example from the Wudinghe River, China. Geogr. Res. 29 (3), 397–407 (in Chinese with English Abstract).
Xue, H.W., 1995. Research on the erosion by rain storm in Zaozigou watershed in Qianxian county. Agric. Res. Arid Areas. 13 (2), 126–131 (in Chinese with English Abstract).
Yang, B.Z., 2003. The height measurement method and the area extend method for measuring sediment retention by check dams. Yellow River 25 (10), 25–26 (in Chinese).
Yang, S.W., Qiu, Z.J., Pan, X.X., Yin, H.M., 1989. Investigation on damage of soil erosion controlling structures during the heavy storm “Aug. 1988” at Tanghu Plateau and the lesson to be drawn down. Soil and Conservation in China 2, 26–29 (in Chinese with English Abstract).
Yang, S.L., Zhang, J., Zhu, J., Smith, J.P., Dai, S.B., Gao, A., Li, P., 2005. Impact of dams on Yangtze River sediment supply to the sea and delta intertidal wetland response. J. Geophys. Res. 110, F03006.
Yang, Z.S., Wang, H.J., Saito, Y., Milliman, J.D., Xu, K.H., Qiao, S.Q., Shi, G.Y., 2006. Dam impacts on the Changjiang (Yangtze) river sediment discharge to the sea: the past 55 years and after the Three Gorges Dam. Water Resour. Res. 42, W044407.
Yang, M., Li, X.Z., Hu, Y.M., He, X.Y., 2007. Annual sediment yield in sub-watersheds at upper reaches of Minjiang River: a simulation with SEDD model. Chin. J. Appl. Ecol. 18 (8), 1758–1764 (in Chinese with English Abstract).
Yellow River Conservancy Commission of MWR, 2016. Yellow River Sediment Bulletin (in Chinese). http://www.yellowriver.gov.cn/nishagonggao/, Accessed date: 24 April 2018.
Yue, S., Pilon, P., Phinney, B., Cavadias, G., 2002. The influencing of autocorrelation on the ability to detect trend in hydrological series. Hydrol. Process. 16 (9), 1807–1829.
Zhang, Y., Liu, B.Y., Shi, P.J., Jiang, Z.S., 2001. Crop cover factor estimating for soil loss prediction. Acta Ecol. Sin. 21 (7), 1050–1056 (in Chinese with English Abstract).
Zhang, W.B., Xie, Y., Liu, B.Y., 2003. Rainfall erosivity estimation using daily rainfall amounts. Sci. Geogr. Sin. 22 (6), 705–711 (in Chinese with English Abstract).
Zhang, K.L., Li, S.C., Peng, W.Y., Yu, B.F., 2004. Erodibility of agricultural soils on the loess plateau of China. Soil Tillage Res. 76 (2), 157–165.
Zhang, Q., Xu, C.Y., Becker, S., Jiang, T., 2006. Sediment and runoff changes in the Yangtze River basin during past 50 years. J. Hydrol. 331, 511–523.
Zhang, L., Shi, C.X., Zhang, H., 2010. Effects of check-dams on sediment storage –release in Chabagou watershed. Transaction of the CSAE 26 (2), 64–69.
Zhang, X.L., Li, Z.R., Zhou, Y.J., Chu, X.J., 2015a. Numerical simulation and analysis of a typical heavy rainfall in east of Northwest China. Journal of Arid Meteorology 33 (4), 616–625 (in Chinese with English Abstract).
Zhang, K.L., Xie, Y., Wei, X., 2015b. Soil Erosion Evaluation in Loess Plateau. Science Press, Beijing (in Chinese).
Zhao, B.L., Niu, Z., 1983. A study on the measurement method and the characteristics of sediment concentration for hyper-concentrated flow in the Yellow River. Hydrology 5, 21–27 (in Chinese).
Zhao, G.J., Mu, X.M., Tian, P., Wang, F., Gao, P., 2012. The variation trend of stream flow and sediment flux in the middle reaches of Yellow River over the past 60 years and the influencing factors. Resources Science 34 (6), 1070–1078 (in Chinese with English Abstract).
Zhao, G.J., Kondolf, G.M., Mu, X.M., Han, M.W., He, Z., Rubin, Z., Wang, F., Gao, P., Sun, W.Y., 2017. Sediment yield reduction associated with land use changes and check dams in a catchment of the loess plateau, China. Catena 148, 126–137.
Zhao, J., Yang, Z., Govers, G., 2019. Soil and water conservation measures reduce soil and water losses in China but not down to background levels: evidences from erosion plot data. Geoderma 337, 729–741.
Zhu, X.M., 1953. A preliminary study on soil erosion and its classification for Dongzhi tableland. New Yellow River 9, 37–40 (in Chinese).
Zhu, X.M., 1954. Soil erosion and its evolution in Jinghe watershed. Acta Pedol. Sin. 2 (4), 209–222 (in Chinese).
Zuo, D.P., Xu, Z.X., Yao, W.Y., Jin, S.Y., Xiao, P.Q., Ran, D.C., 2016. Assessing the effects of changes in land use and climate on runoff and sediment yields from a watershed in the Loess Plateau of China. Sci. Total Environ. 544, 238–250.